Efficient Sensitivity Calculation for Insulation Systems in HVDC Cable Joints

[1,2]M. Greta Ruppert, [1,2]Yvonne Späck-Leigsnering, [3]Myriam Koch, [1,2]Herbert De Gersem

[1] *Technische Universität Darmstadt, Institute for Accelerator Science and Electromagnetic Fields, Schlossgartenstr. 8, 64289 Darmstadt, Germany*
[2] *Technische Universität Darmstadt, Graduate School of Computational Engineering Dolivostraße 15, 64293 Darmstadt, Germany*
[3] *Technische Universität München, Professorship for High Voltage Engineering and Switchgear Technology, Arcisstr. 21, 80333 München, Germany*

Abstract Many high voltage direct current cable systems include field grading materials with can be mixed such that the properties can be tailored to the particular configuration. This comes with a drastic increase in the number of design parameters to be considered in the nonlinear transient electrothermal finite element model. This paper introduces the adjoint variable method to efficiently calculate the sensitivities of the quantities of interest with respect to a large set of design parameters.

1. Introduction

The development of high voltage direct current (HVDC) cable systems is one of the greatest challenges of our time for the high voltage engineering community [1–3]. Cable joints are known to be a particularly vulnerable part of these systems [1, 4–6]. Field strengths in the range of several kV/mm must be balanced carefully, as they may otherwise lead to a dielectric breakdown of the insulating material. A remedy is the resistive field control, i.e. a nonlinear field grading material (FGM) layer that is inserted along critical interfaces [4, 7–9]. This material features a strongly nonlinear conductivity, similar to the overvoltage clipping of metal-oxide surge arresters [10, 11]. Advances in the development of FGM allow to individually tailor its characteristics to the respective application [12, 13]. However, at the moment, engineers are mainly guided by rules of thumb, by know-how and previous experience. So far, only few systematic investigations studied the different design parameters of the FGMs based on field simulation and laboratory experiments [7, 13, 14].

The design process of FGMs is complicated by the large number of possible parameter configurations. A remedy is utilization of sensitivity information. Sensitivities, or gradients, describe how and how strong a quantity of interest (QoI) is influenced by a design parameter at a given working point. Different methods for the computation of sensitivities in field simulation settings are known. In contrast to the commonly used finite differences or the direct sensitivity method (DSM) [15, 16], the adjoint variable method (AVM) has computational costs that are nearly independent of the number of parameters [15–17]. In electrical engineering, the AVM has been applied to microwave engineering problems [16, 18–22] and for a linear electroquasistatic problem in frequency domain [23]. However, the AVM has not been applied to the nonlinear electrothermal cable joint problem. This work presents the AVM formulation for coupled electrothermal problems with nonlinear media at steady state. The method is applied to a 320 kV cable joint specimen and the results are validated using the DSM as a reference.

2. Modeling and Solution Approach

2.1. Cable Joint Specimen

Figure 1 shows the cross section of the investigated 320 kV HVDC cable joint specimen in the ρ-z-plane. The total length of the joint is 1.4 m. Two copper conductors of 2000 mm^2 cross section (domain 1) are linked by an aluminum connector (domain 2). These domains are covered by a layer of conductive silicone rubber (SiR) (domain 3). The cable insulation consists of 26 mm thick cross-linked polyethylene (XLPE) (domain 4) and the joint insulation of an insulating SiR (domain 5). Both insulating domains are separated by a nonlinear resistive FGM layer (domain 6, highlighted in orange). The outer cable sheath (domain 7) and joint sheath (domain 8) are on ground potential. The joint is surrounded by a 30 cm thick sand foundation and is buried two meters below the ground. The joint is subjected to continuous grid operation, i.e. an excitation of 320 kV is applied. The conductors, the conductive SiR covering the conductors and the conductor clamp are modeled as a perfect electric conductors. Furthermore, a conductor temperature of 65°C is assumed [14].

For failures of the cable joint, the tangential field strength along the material boundary between XLPE and FGM is particularly critical [7]. Along this interface, the maximum tangential field stress occurs in the proximity of the triple point next to the conductor clamp, as indicated by the red circle in Fig. 1.

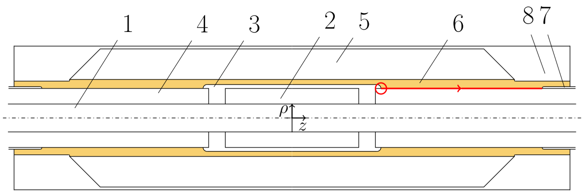

Figure 1 – Schematic of the investigated HVDC joint [7] in the ρ-z-plane (drawing is not to scale). The typical position of the maximum tangential field along the interface of XLPE and FGM is marked by a red circle. The numbers indicate the different materials as described in the text, the nonlinear FGM is highlighted in orange.

2.2. Nonlinear Field Grading Material

The conductivity of the FGM is described by the analytic function [7]

$$\sigma(E,T) = p_1 \frac{1+p_4^{(E-p_2)\,p_2^{-1}}}{1+p_4^{(E-p_3)\,p_2^{-1}}} \cdot \exp\left(-p_5\left(T^{-1}-T_0^{-1}\right)\right), \tag{1}$$

where E denotes the magnitude of the electric field strength in V/m and T is the temperature in K. The parameters are $p_1 = 10^{-10}$ S/m, $p_2 = 0.7 \cdot 10^6$ V/m, $p_3 = 2.4 \cdot 10^6$ V/m, $p_4 = 1864$ and $p_5 = 3713.59$ K and $T_0 = 293.15\,K$. The field-dependence at a fixed temperature is shown in Fig. 2. The remaining material properties are summarized in Table 1.

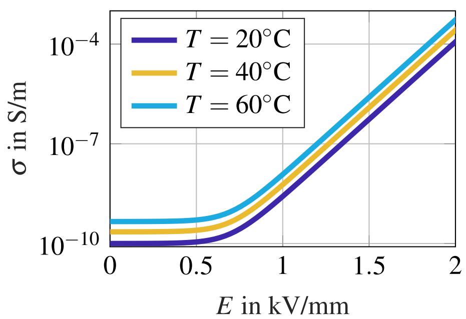

Figure 2 – Nonlinear field-dependent conductivity of the FGM. The FGM conductivity is described by the analytic function (1).

Table 1 – HVDC cable joint material parameters

Material	σ in S/m	λ in W/(m· K)
conductive SiR(3)	–	0.25
XLPE (4)	10^{-15}	0.3
insulating SiR (5)	$5 \cdot 10^{-13}$	0.22
FGM (6)	see (1)	0.5
outer cable sheath (7)	–	0.25
outer joint sheath (8)	–	0.25
sand	–	0.54
soil	–	0.79

2.3. Electrothermal Modeling and Numerical Approach

The electrothermal behavior of cable joints during steady state operation can be described by the combination of the stationary current equation and the heat conduction equation. The stationary current equation reads

$$-\operatorname{div}(\sigma \operatorname{grad}(\phi)) = 0 \qquad \boldsymbol{r} \in \Omega, \tag{2a}$$
$$\phi = \phi_{\text{fixed}} \qquad \boldsymbol{r} \in \Gamma_{\text{D, el}}, \tag{2b}$$
$$-\sigma \operatorname{grad}(\phi) \cdot \boldsymbol{n}_{\text{el}} = 0 \qquad \boldsymbol{r} \in \Gamma_{\text{N, el}}, \tag{2c}$$

where ϕ is the electric scalar potential and σ is the electric conductivity. The position vector is denoted as $\boldsymbol{r}$, Ω is the computational domain. ϕ_{fixed} is the fixed potential at the electrodes, $\Gamma_{\text{D, el}} \neq \emptyset$, and $\boldsymbol{n}_{\text{el}}$ is the unit vector at the Neumann boundaries, $\Gamma_{\text{N, el}} = \partial\Omega \backslash \Gamma_{\text{D, el}}$. The stationary heat conduction equation reads

$$-\operatorname{div}(\lambda \operatorname{grad}(T)) = \dot{q} \qquad \boldsymbol{r} \in \Omega, \tag{3a}$$
$$T = T_{\text{fixed}} \qquad \boldsymbol{r} \in \Gamma_{\text{D, th}}, \tag{3b}$$
$$-\lambda \operatorname{grad}(T) \cdot \boldsymbol{n}_{\text{th}} = 0 \qquad \boldsymbol{r} \in \Gamma_{\text{N, th}}, \tag{3c}$$

where λ is the thermal conductivity. T_{fixed} are the fixed temperatures at the Dirichlet boundaries, $\Gamma_{\text{D, th}} \neq \emptyset$, and $\boldsymbol{n}_{\text{th}}$ is the unit vector at the Neumann boundaries, $\Gamma_{\text{N, th}} = \partial\Omega \backslash \Gamma_{\text{D, th}}$. The two equations are coupled along the Joule losses $\dot{q} = \sigma |\operatorname{grad}(\phi)|^2$ and the temperature-dependence of the electric conductivity, $\sigma = \sigma(E,T)$.

Both equations, (2) and (3), are formulated as a two-dimensional (2D) axisymmetric Finite Element (FE) problem using linear nodal shape functions. The coupling between the two systems is handled by a damped successive substitution method where in each iteration the nonlinearity of the electric subproblem is solved using the Newton method. The simulation is performed with a mesh consisting of 51681 nodes and 106113 elements. The implementation is carried out in the in-house FE solver *Pyrit*, which is in the following refered to as HVDC solver.

2.4. Solver Validation

For the validation of the HVDC solver, the simulation results of the steady state are compared to simulation results obtained via COMSOL Multiphysics®. Fig. 3 shows the tangential electric field distribution, E_{tan}, and Fig. 4 the temperature distribution along the interface between the XLPE and the FGM (see red line in Fig. 1). A perfect agreement of the results of the HVDC solver and the reference solution is obtained.

3. Sensitivity Calculation

FGM can be compiled in different compositions. Thereby, the characteristic may be taylored to the desired properties of the joint, which corresponds to an optimization of the parameters p_1 to p_5 of (1). Although five parameters do not sound like much at first, one quickly reaches its limits when manually optimizing them. For example, the investigation of only three values

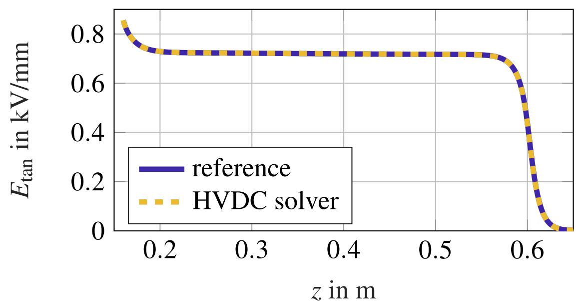

Figure 3 – Tangential electric field strength, $E_{\tan}$, along the interface between XLPE and FGM.

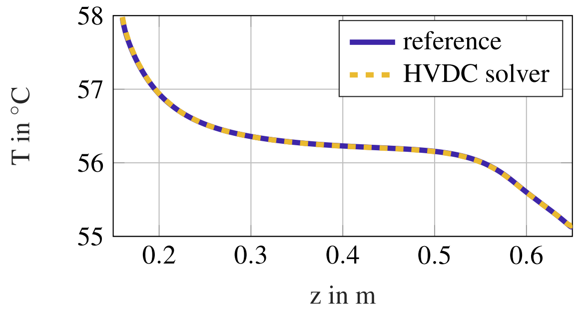

Figure 4 – Temperature, T, along the interface between XLPE and FGM.

for each parameter leads to more than 240 possible combinations, which need to be simulated in a parameter sweep. In an optimization task, the number of expensive FE simulation runs can be effectively reduced by the utilization of sensitivity information [24]. Sensitivities describe the influence a design parameter p_j, $j = 1,\dots,N_\mathrm{P}$, has on a given QoI $G_k(\phi,T)$, $k = 1,\dots,N_\mathrm{QoI}$. In the scope of this work, they are defined as the derivative of the QoI with respect to the paramter, i.e. $\frac{\mathrm{d}G_k}{\mathrm{d}p_j}(\boldsymbol{p}_0)$, where $\boldsymbol{p}_0$ is the current parameter configuration.

3.1. Direct Sensitivity Method

One of the most common methods for sensitivity calculation is the DSM [16]. For the DSM, the sensitivities are written in more detail using the chain rule,

$$\frac{\mathrm{d}G_k}{\mathrm{d}p_j}(\boldsymbol{p}_0) = \frac{\partial G_k}{\partial p_j}(\boldsymbol{p}_0) + \frac{\partial G_k}{\partial \phi}\frac{\mathrm{d}\phi}{\mathrm{d}p_j}(\boldsymbol{p}_0) + \frac{\partial G_k}{\partial T}\frac{\mathrm{d}T}{\mathrm{d}p_j}(\boldsymbol{p}_0), \quad (4)$$

where the sensitivities of the solution, i.e. $\frac{\mathrm{d}\phi}{\mathrm{d}p_j}(\boldsymbol{p}_0)$ and $\frac{\mathrm{d}T}{\mathrm{d}p_j}(\boldsymbol{p}_0)$, are typically unknown. The DSM computes these missing terms by taking the derivative of (2) and (3) with respect to p_j and solving the arising system of coupled linear partial differential equations (PDEs) for $\frac{\mathrm{d}\phi}{\mathrm{d}p_j}(\boldsymbol{p}_0)$ and $\frac{\mathrm{d}T}{\mathrm{d}p_j}(\boldsymbol{p}_0)$. The sensitivity of the QoIs are then computed directly using (4). Therefore, the DSM requires the solution of one additional coupled system of linear PDEs for each parameter. This is the reason why the method is disadvantageous for problems with a large parameter space such as HVDC cable joints.

3.2. Adjoint Variable Method

The AVM on the other hand, is a sensitivity computation method that is extremely efficient when the number of parameters, N_P, is larger than the number of QoIs, N_QoI [15, 17]. Its idea is to avoid the computation of $\frac{\mathrm{d}\phi}{\mathrm{d}p_j}$ and $\frac{\mathrm{d}T}{\mathrm{d}p_j}$ by formulating the QoIs cleverly [15, 17]: The QoIs are expressed in terms of a functional g_k, which is integrated over the computational domain, Ω. In addition, the nonlinear stationary current problem (2) as well as the heat conduction problem (3) are embedded, multiplied by test functions $w_{\mathrm{el},k}(\boldsymbol{r})$ and $w_{\mathrm{th},k}(\boldsymbol{r})$, respectively, i.e.

$$\begin{aligned} G_k(\phi,T,\boldsymbol{p}) = &\int_\Omega g_k(\phi,T,\boldsymbol{r},\boldsymbol{p})\,\mathrm{d}\Omega \\ &- \int_\Omega w_{\mathrm{el},k}(\boldsymbol{r})\underbrace{\left(-\operatorname{div}\left(\sigma\operatorname{grad}(\phi)\right)\right)}_{=0}\mathrm{d}\Omega \\ &- \int_\Omega w_{\mathrm{th},k}(\boldsymbol{r})\underbrace{\left(-\operatorname{div}\left(\lambda\operatorname{grad}(\phi)\right)+\dot{q}\right)}_{=0}\mathrm{d}\Omega\,. \end{aligned} \quad (5)$$

For any ϕ and T solving (2) and (3), the additional terms are zero and the test functions can be chosen freely. The goal of the AVM is to choose the test functions in such a way, that the sensitivity of the extended QoI no longer contains the unknown terms $\frac{\mathrm{d}\phi}{\mathrm{d}p_j}$ and $\frac{\mathrm{d}T}{\mathrm{d}p_j}$. After a lengthy derivation, it can be shown that the unknown term is eliminated if the test functions are chosen as the adjoint variables, i.e. the solution of the so-called adjoint problem [15, 17]. The adjoint problem for electrothermal HVDC problems with nonlinear parameter-dependent materials, i.e. $\sigma(E(\boldsymbol{p}),T(\boldsymbol{p}),\boldsymbol{p})$ and $\lambda(T(\boldsymbol{p}),\boldsymbol{p})$, is given by the coupled system of linear PDEs:

$$\begin{aligned} &-\operatorname{div}\left(\boldsymbol{\sigma}_\mathrm{d}\operatorname{grad}\left(w_{\mathrm{el},k}\right)\right) \\ &+\operatorname{div}\left(w_{\mathrm{th},k}(\boldsymbol{\sigma}_\mathrm{d}+\sigma\mathbf{1})\operatorname{grad}(\phi)\right) = \frac{\mathrm{d}g_k}{\mathrm{d}\phi}, \quad \boldsymbol{r}\in\Omega; \end{aligned} \quad (6a)$$

$$w_{\mathrm{el},k} = 0, \quad \boldsymbol{r}\in\Gamma_{\mathrm{D,el}}; \quad (6b)$$

$$-\boldsymbol{\sigma}_\mathrm{d}\operatorname{grad}\left(w_{\mathrm{el},k}\right)\cdot\boldsymbol{n}_\mathrm{el} = 0, \quad \boldsymbol{r}\in\Gamma_{\mathrm{N,el}}; \quad (6c)$$

and

$$\begin{aligned} &\operatorname{grad}\left(w_{\mathrm{el},k}\right)\frac{\partial\sigma}{\partial T}\operatorname{grad}(\phi) + \operatorname{grad}(w_{\mathrm{th},k})\frac{\partial\lambda}{\partial T}\operatorname{grad}(T) \\ &-\operatorname{div}\left(\lambda\operatorname{grad}\left(w_{\mathrm{th},k}\right)\right) - w_{\mathrm{th},k}\frac{\partial\sigma}{\partial T}E^2 = \frac{\mathrm{d}g_k}{\mathrm{d}T}, \quad \boldsymbol{r}\in\Omega; \end{aligned} \quad (7a)$$

$$w_{\mathrm{th},k} = 0, \quad \boldsymbol{r}\in\Gamma_{\mathrm{D,th}}; \quad (7b)$$

$$-\boldsymbol{\lambda}\operatorname{grad}\left(w_{\mathrm{th},k}\right)\cdot\boldsymbol{n}_\mathrm{th} = 0, \quad \boldsymbol{r}\in\Gamma_{\mathrm{N,th}}; \quad (7c)$$

where all quantities are evaluated at the current parameter configuration $\boldsymbol{p}_0$. The identity tensor is denoted by $\mathbf{1}$ and the differential conductivity tensor by

$$\begin{aligned} \boldsymbol{\sigma}_\mathrm{d}(\boldsymbol{E},T) = &\frac{\mathrm{d}\boldsymbol{J}}{\mathrm{d}\boldsymbol{E}} \\ = &\sigma(E,T)\mathbf{1} + 2\frac{\mathrm{d}\sigma}{\mathrm{d}E^2}(E,T)\begin{bmatrix} E_\rho E_\rho & E_\rho E_z \\ E_z E_\rho & E_z E_z \end{bmatrix}, \end{aligned} \quad (8)$$

where E_ρ and E_z denote the ρ and z component of the electric field $\boldsymbol{E}$, respectively.

Once the electric potential, the temperature and the adjoint variables, $w_{\mathrm{el},k}$ and $w_{\mathrm{th},k}$, are available, the sensitivity with respect to any parameter can be computed directly by

$$\begin{aligned}\frac{\mathrm{d}G_k}{\mathrm{d}p_j}(\boldsymbol{p}_0) = \int_\Omega \frac{\partial g_k}{\partial p_j}\,\mathrm{d}\Omega + \int_\Omega w_{\mathrm{th},k}\frac{\partial \sigma}{\partial p_j}E^2\,\mathrm{d}\Omega \\ - \int_\Omega \operatorname{grad}\left(w_{\mathrm{el},k}\right)\frac{\partial \sigma}{\partial p_j}\operatorname{grad}(\phi)\,\mathrm{d}\Omega \\ - \int_\Omega \operatorname{grad}\left(w_{\mathrm{th},k}\right)\frac{\partial \lambda}{\partial p_j}\operatorname{grad}(T)\,\mathrm{d}\Omega.\end{aligned} \tag{9}$$

Again, all quantities are evaluated for the current parameter configuration $\boldsymbol{p}_0$.

Note that the coupled adjoint system (6) and (7) does not depend on the parameter p_j, so that the same test functions or adjoint variables, $w_{\mathrm{el},k}$ and $w_{\mathrm{th},k}$, can be used to compute the sensitivity of G_k with respect to any parameter. Thus, the AVM method requires the solution of only one additional linear coupled system of PDEs, independent of the number of parameters. In case of the cable joint, this means that the AVM is able to compute the sensitivity of any QoI with respect to all 15 material parameters (five parameters determining the nonlinearity of (1) and ten parameters defined in Table 1) using only one additional linear coupled simulation, whereas the DSM would require 15 additional simulations.

4. Results

The adjoint formulation (6) and (7) is validated by comparing the sensitivities obtained via the AVM to the results of the DSM. According to (5), the QoIs must be expressed in terms of a functional, g_k, that is integrated over the computational domain, i.e.

$$G_k(\phi, T, \boldsymbol{p}) = \int_\Omega g_k(\phi, T, \boldsymbol{r}, \boldsymbol{p})\,\mathrm{d}\Omega.$$

To demonstrate that this integral notation is not a restriction in the choice of QoIs, the validation is performed for both an integrated QoI as well as for a QoI evaluated at a specific position. The sensitivity of both QoIs is computed with respect to the parameter p_2 of (1), which determines at which field strength the conductivity of the FGM switches from the base conductivity to the strongly nonlinear region (see Fig. 5).

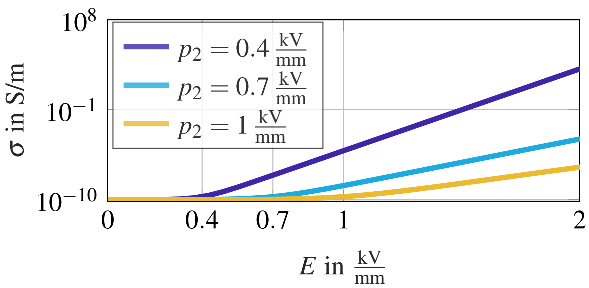

Figure 5 – Field-dependence of the nonlinear conductivity defined by (1) for different values of p_2.

As an exampled for an integrated QoI, the Joule losses inside the insulation of the cable joint, i.e.

$$P_{\mathrm{loss}} = \int_\Omega \sigma|\operatorname{grad}(\phi)|^2\,\mathrm{d}\Omega,$$

are considered. Figure 6a shows that increasing p_2 leads to a reduction of the Joule losses. The reason is that a later transition into the nonlinear region results in lower conductivities and, thus, lower losses. Figure 6b shows the sensitivity of the Joule losses with respect to p_2 for different values of p_2. The negative signs of the sensitivities confirm that an increase of p_2 reduces the losses. Furthermore, the absolute values of the sensitivities show that P_{loss} is particularly sensitive for small values of p_2. It can be seen that for this integrated QoI, the validation is successful and the results of the AVM are in perfect agreement with those of the DSM.

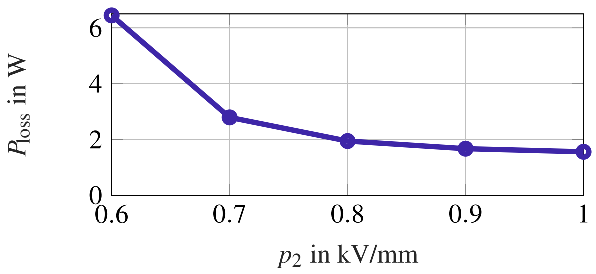

(a)

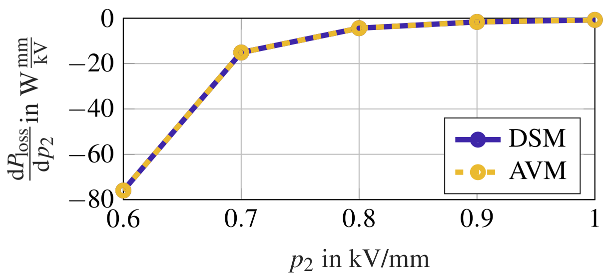

(b)

Figure 6 – (a) Joule losses, P_{loss}, for different values of p_2. (b) Sensitivity of the Joule losses with respect to p_2, $\frac{\mathrm{d}P_{\mathrm{loss}}}{\mathrm{d}p_2}$, for different values of p_2.

The second QoI is the tangential field stress, E_{crit}, located at the position, $\boldsymbol{r}_{\mathrm{crit}}$, next to the conductor clamp (see indicated position in Fig. 2). The evaluation of the electric field at $\boldsymbol{r}_{\mathrm{crit}}$ can be expressed by the Dirac delta function $\delta(\boldsymbol{r} - \boldsymbol{r}_{\mathrm{crit}})$,

$$E_{\mathrm{crit}} = \int_\Omega E_{\mathrm{tan}}\delta(\boldsymbol{r} - \boldsymbol{r}_{\mathrm{crit}})\,\mathrm{d}\Omega.$$

Figure 7a shows that small values of p_2 reduce the critical field strength. Since small values of p_2 simultaneously increase the Joule losses, there is a clear trade-off between good field grading and low losses, which is typical of nonlinear resistive field grading [14, 25]. Figure 7b shows that, again, a perfect agreement between the AVM and the DSM is obtained. The adjoint formulation presented in Sec. 3.2 has, thus, been successfully validated.

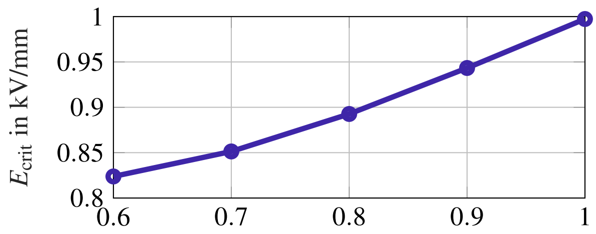

(a)

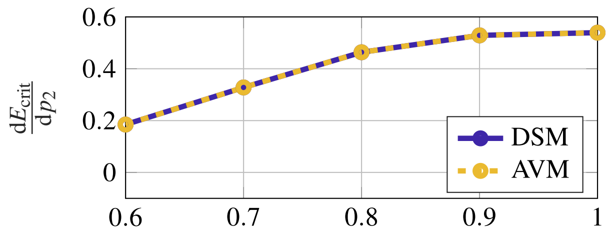

(b)

Figure 7 – (a) Critical field stress E_{crit}, for different values of p_2. (b) Sensitivity of the critical field stress with respect to p_2, $\frac{\mathrm{d}E_{\mathrm{crit}}}{\mathrm{d}p_2}$, for different values of p_2.

5. Conclusion

The behavior of a high voltage direct current cable joint is influenced by a large number of design parameters, in particular by the material parameters of the field grading material layer. When optimizing the joint performance, the availability of sensitivities allows to significantly reduce the number of finite element simulation solver calls. This work proposes the adjoint variable method for calculating sensitivities of important quantities of interest with respect to a set of design parameters. The adjoint variable method was formulated for coupled electrothermal high voltage direct current problems with nonlinear material characteristics. The coupled system of adjoint partial differential equations is presented and it is shown how to consider quantities of interest that are evaluated at specific positions. The method was successfully applied to a 320 kV cable joint featuring a resistive field grading layer. It was discussed that the adjoint variable method's computational costs are nearly independent of the number of design parameters. This is particularly beneficial for the optimization of cable joints, which needs to consider a large parameter space.

6. Acknowledgements

The authors thank Rashid Hussain for providing the simulation model and material characteristics published in [7], and Julian Buschbaum and Jonas Bundschuh for the helpful discussions.
This work is supported by the Graduate School CE within the Centre for Computational Engineering at the Technische Universität Darmstadt.

7. References

[1] Cigré Working Group D1.56. *Field grading in electrical insulation systems*. Technical Brochure TB794. Conseil international des grands réseaux électriques, 2020.

[2] Hossein Ghorbani, Marc Jeroense, Carl-Olof Olsson, and Markus Saltzer. HVDC cable systems—highlighting extruded technology. *IEEE Transactions on Power Delivery*, 29(1):414–421, 2014.

[3] Frank Messerer. Current challenges in energy policy. In *HVDC Cable Systems Symposium: Theory and Practice*, online, Germany, January 2022.

[4] George Chen, Miao Hao, Zhiqiang Xu, Alun Vaughan, Junzheng Cao, and Haitian Wang. Review of high voltage direct current cables. *CSEE Journal of Power and Energy Systems*, 1(2):9–21, 2015.

[5] Christoph Jörgens and Markus Clemens. A review about the modeling and simulation of electro-quasistatic fields in HVDC cable systems. *Energies*, 13(19):5189, 2020.

[6] Stephan Pöhler and Roland Dongping Zhang. Prequalification test for extruded 525kV HVDC cable systems – SuedLink and SuedOstLink. In *HVDC Cable Systems Symposium: Theory and Practice*, online, Germany, January 2022.

[7] Rashid Hussain and Volker Hinrichsen. Simulation of thermal behavior of a 320 kV HVDC cable joint with nonlinear resistive field grading under impulse voltage stress. In *CIGRÉ Winnipeg 2017 Colloquium*, 2017.

[8] Thomas Christen, Lise Donzel, and Felix Greuter. Nonlinear resistive electric field grading part 1: Theory and simulation. *IEEE Electrical Insulation Magazine*, 26(6):47–59, November 2010.

[9] Thomas Christen. Nonlinear electric conduction and resistive field control. In *HVDC Cable Systems Symposium: Theory and Practice*, online, Germany, January 2022.

[10] Volker Hinrichsen. *Metal-Oxide Surge Arresters in High-Voltage Power Systems - Fundamentals*. Siemens AG, 3rd edition, 2011.

[11] Yvonne Späck-Leigsnering, M. Greta Ruppert, Erion Gjonaj, Herbert De Gersem, and Volker Hinrichsen. Simulation analysis of critical parameters for thermal stability of surge arresters. *IEEE Transactions on Power Delivery*, page 1, 2021.

[12] Johann Bauer, Albert Claudi, Stefan Kornhuber, Stefan Kühnel, Jens Lambrecht, and Sebastian Wels. Silicon-Gel-Compound für die Nichtlinear-Resistive Feldsteuerung –zur technischen Anwendung und Auslegung des Isoliersystems. In *VDE ETG – Fachtagung Hochspannungstechnik 2020*, Berlin, November 2020.

[13] Maximilian Secklehner, Rashid Hussain, and Volker Hinrichsen. Tailoring of new field grading materials for HVDC systems. In *2017 INSUCON – 13th International Electrical Insulation Conference (INSUCON)*. IEEE, May 2017.

[14] Yvonne Späck-Leigsnering, M. Greta Ruppert, Erion Gjonaj, Herbert De Gersem, and Myriam Koch. Towards electrothermal optimization of a HVDC cable joint based on field simulation. *Energies*, 14(10):2848, May 2021.

[15] Shengtai Li and Linda Petzold. Adjoint sensitivity analysis for time-dependent partial differential equations with adaptive mesh refinement. *Journal of Computational Physics*, 198(1):310–325, July 2004.

[16] N.K. Nikolova, J.W. Bandler, and M.H. Bakr. Adjoint techniques for sensitivity analysis in high-frequency structure CAD. *IEEE Transactions on Microwave Theory and Techniques*, 52(1):403–419, January 2004.

[17] Yang Cao, Shengtai Li, Linda Petzold, and Radu Serban. Adjoint sensitivity analysis for differential-algebraic equations: The adjoint DAE system and its numerical solution. *SIAM Journal on Scientific Computing*, 24(3):1076–1089, January 2003.

[18] N.K. Georgieva, S. Glavic, M.H. Bakr, and J.W. Bandler. Feasible adjoint sensitivity technique for EM design optimization. *IEEE Transactions on Microwave Theory and Techniques*, 50(12):2751–2758, December 2002.

[19] F. Alessandri, M. Mongiardo, and R. Sorrentino. New efficient full wave optimization of microwave circuits by the adjoint network method. *IEEE Microwave and Guided Wave Letters*, 3(11):414–416, November 1993.

[20] Mohamed H. Bakr, Osman S. Ahmed, Mohamed H. El Sherif, and Tsuyoshi Nomura. Time domain adjoint sensitivity analysis of electromagnetic problems with nonlinear media. *Optics Express*, 22(9):10831, April 2014.

[21] Il-Han Park, In-Gu Kwak, Hyang-Beom Lee, Song-Yop Hahn, and Ki-Sik Lee. Design sensitivity analysis for transient eddy current problems using finite element discretization and adjoint variable method. *IEEE Transactions on Magnetics*, 32(3):1242–1245, May 1996.

[22] Christopher M. Lalau-Keraly, Samarth Bhargava, Owen D. Miller, and Eli Yablonovitch. Adjoint shape optimization applied to electromagnetic design. *Optics Express*, 21(18):21693, September 2013.

[23] D. Zhang, F. Kasolis, and M. Clemens. Topology optimization for a station class surge arrester. In *The 12th International Symposium on Electric and Magnetic Fields (EMF 2021)*, 2021.

[24] Ion Gabriel Ion, Zeger Bontinck, Dimitrios Loukrezis, Ulrich Römer, Oliver Lass, Stefan Ulbrich, Sebastian Schöps, and Herbert De Gersem. Deterministic optimization methods and finite element analysis with affine decomposition and design elements. *Electrical Engineering*, 100(4):2635–2647, December 2018.

[25] Thi Thu Nga Vu, Gilbert Teyssedre, and Séverine Le Roy. Electric field distribution in HVDC cable joint in non-stationary conditions. *Energies*, 14(17):5401, 2021.